


A motor independent requirement for dynein light chain in *Caenorhabditis elegans* meiotic synapsis

Sara M. Fielder,^{1,2,†,‡} Tori Kent,¹ Huiping Ling,¹ Elizabeth J. Gleason,¹ and William G. Kelly ^{1,*}

¹Biology Department, Emory University, Atlanta, GA 30322, USA and

²Program in Genetics and Molecular Biology, Emory University, Atlanta, GA 30322, USA

[†]Present address: Department of Pediatrics, Washington University in St. Louis School of Medicine, Saint Louis, MI 63110, USA.

[‡]Present address: *C. elegans* Model Organism Screening Center, Washington University in St. Louis School of Medicine, Saint Louis, MI 63110, USA.

*Corresponding author: Biology Department, Emory University, 1510 Clifton Rd. NE, Atlanta, GA 30322, USA. Email: bkelly@emory.edu

Abstract

The dynein motor complex is thought to aid in homolog pairing in many organisms by moving chromosomes within the nuclear periphery to promote and test homologous interactions. This precedes synaptonemal complex (SC) formation during homolog synapsis, which stabilizes homolog proximity during recombination. We observed that depletion of the dynein light chain (DLC-1) in *Caenorhabditis elegans* irreversibly prevents synapsis, causing an increase in off-chromatin formation of SC protein foci with increasing temperature. This requirement for DLC-1 is independent of its function in dynein motors, as SYP protein foci do not form with depletion of other dynein motor components. In contrast to normal SC-related structures, foci formed with DLC-1 depletion are resistant to dissolution with 1,6-hexanediol, similar to aggregates of SC proteins formed in high growth temperatures. Dynein light chains have been shown to act as hub proteins that interact with other proteins through a conserved binding motif. We identified a similar DLC-1 binding motif in the *C. elegans* SC protein SYP-2, and mutation of the putative motif causes meiosis defects that are exacerbated by elevated temperatures. We propose that DLC-1 acts as a pre-synapsis chaperone-like factor for SYP proteins to help regulate their self-association prior to the signals for SC assembly, a role that is revealed by its increased essentiality at elevated temperatures.

Keywords: meiosis; meiotic synapsis; dynein light chain; *C. elegans*

Introduction

Meiotic synapsis physically aligns and holds homologous chromosomes together during meiosis to aid in recombination, ensuring inheritance of the correct chromosome complement in offspring. The synaptonemal complex (SC) is a conserved structure composed of an axis that assembles onto Cohesin proteins on each chromosome, and a central element (CE) that physically connects two homologs together [reviewed in [Lui and Colaiacovo \(2013\)](#)]. The CE in *Caenorhabditis elegans* consists of six SYP proteins that assemble onto the axial element of the SC after homologous chromosomes have correctly paired ([MacQueen et al. 2002](#); [Colaiacovo et al. 2003](#); [Smolikov et al. 2007, 2009](#); [Schild-Prufert et al. 2011](#); [Hurlock et al. 2020](#)). SYP proteins are prone to inter-protein interactions, and will self-assemble into SC-like structures even if they are unable to assemble onto chromosomes. For example, in mutants lacking either axial element HTP-3 or HIM-3, SYP proteins assemble into nucleoplasmic foci unassociated with chromosomes ([Couteau et al. 2004](#); [Goodyer et al. 2008](#)). These foci, termed *polycomplexes*, are composed of clusters of ladder-like structures, when viewed by electron microscopy, that resemble the normal SC structure between synapsed chromosomes ([Rog et al. 2017](#)). Both the normal SC assembled between homologs and the polycomplexes formed in *htp-3* mutants can be

reversibly disrupted by addition of an amphiphilic solvent, such as 1,6-hexanediol ([Rog et al. 2017](#)). SC protein foci are also observed in the nucleoplasm of animals grown at elevated temperatures above 26.5°C ([Bilgir et al. 2013](#)), but these foci are resistant to solvent ([Rog et al. 2017](#)). This suggests that a structural change in SC proteins occurs at elevated temperatures that prevents their proper assembly onto either chromatin or into polycomplexes.

In *C. elegans*, chromosomes initially pair using Zinc-finger In Meiosis (ZIMs) proteins that bind specific sequence repeats located on one end of each chromosome ([Phillips et al. 2005](#); [Phillips and Dernburg 2006](#)). This end then localizes to the nuclear envelope and connects indirectly to the dynein motors in the cytoplasm through the nuclear membrane proteins SUN-1 and ZYG-12 ([Penkner et al. 2007](#); [Sato et al. 2009](#)). Dynein is thought to aid chromosomes in the search for their homologous pairing partners by moving chromosomes around the nuclear periphery and increasing their interactions ([Sato et al. 2009](#); [Wynne et al. 2012](#)). A current model is that potential homolog matches are tested through dynein-dependent forces that can disrupt nonhomologous associations, with correct matches providing tension-dependent signals for synapsis initiation ([Sato et al. 2009](#)). However, mutants lacking dynein dependent movement or all pairing center activity can still undergo nonhomologous and fold-back synapsis, indicating that synapsis can still occur

Received: August 25, 2021. Accepted: October 29, 2021

© The Author(s) 2021. Published by Oxford University Press on behalf of Genetics Society of America. All rights reserved.

For permissions, please email: journals.permissions@oup.com

without dynein (Penkner et al. 2007; Harper et al. 2011; Rog and Dernburg 2015).

In addition to their identification as a critical component of the dynein motors, dynein light chains has been shown to have many other cellular roles in protein–protein interactions [reviewed in Rapali et al. (2011)]. Light chain dimers bind to specific motifs on other proteins (Rodriguez-Crespo et al. 2001), which are frequently located adjacent to a coiled-coil domain. Light chain binding has been shown to facilitate protein–protein interactions and influence the conformation of its target proteins (Makokha et al. 2002; Nyarko et al. 2004; Wagner et al. 2006) [and reviewed in Rapali et al. (2011)].

In this study, we identify a dynein-independent role for the *C. elegans* dynein light chain (DLC-1) in meiotic synapsis. Depletion of DLC-1 alone causes amphiphilic solvent-resistant foci of SYP proteins, similar to aggregates induced by high temperature, whereas mutation or knockdown of other dynein components does not. DLC-1 is dispensable for SC assembly at lower temperatures, but its absence causes an increased frequency of aggregate formation as the temperature rises. The temperature-dependent requirement for DLC-1 in SC assembly is only observed in oogenic germlines, indicating a sex-specific requirement for its function. We identified a possible DLC-1 interacting motif in the CE protein SYP-2 and show that mutations in this binding site cause meiotic defects that correlate with decreased stability of SYP-2. These results indicate that in addition to its role in dynein-dependent chromosome movement, DLC-1 also interacts with SYP-2 in a manner that influences both its stability and SC protein interactions during SC assembly at elevated temperatures.

Methods

Strains

Strains used in this study are UMT281 (jmntSi13 [pME4.1] II; unc-119(ed3) III dlc-1 prom::3XFLAG::dlc-1::dlc-1 3'UTR (Wang et al. 2016); dlc-1(tm3153) III, syp-2(ok307) V; wglIs227 [syp-2::TY1::EGFP::3xFLAG(92C12) + unc-119(+), dhc-1(or195) I, and dnc-1(or676) IV. Transgenic strains ck38 and ck39 were produced using CRISPR-Cas9 system, discussed below. Animals were grown at temperatures indicated in each figure. Some strains were provided by the CGC, which is funded by NIH Office of Research Infrastructure Programs (P40 OD010440). The UMT281 strain was crossed to the *dlc-1(tm3153)* strain to yield a *dlc-1* deletion strain rescued with the FLAG-tagged DLC-1. This strain was further crossed with the ck38 and ck39 CRISPR allele strains to yield strains KW1500 [FLAG::dlc-1 jmntSi13(pME4.1) II; dlc-1(tm3153) III; syp-2::GFP(ck38) V and KW1501 (FLAG::dlc-1 jmntSi13[pME4.1] II; dlc-1(tm3153) III; AMTA mutant syp-2::GFP(ck39) V.

Transgenic strain construction using CRISPR-Cas9 system

The ck38 (denoted WT *syp-2::GFP*) and ck39 (denoted *syp-2::GFP(AMTA)*) alleles were generated using the CRISPR-Cas9 system. gRNA was designed within 35 bp of site of integration using the IDT design custom gRNA online tool (Table 1). gBlock® Gene Fragment (Integrated DNA Technologies) was amplified using Platinum Super Fi PCR Master Mix (Invitrogen #12358010) with only 12 cycles of PCR to ensure lower chance of incorporation of a mutation into the HDR template. Nine PCR reactions were pooled and purified using the Zymo DNA Clean & Concentrator-5 kit (Zymo D4004). Each Alt-R® CRISPR-Cas9 sgRNA (Integrated DNA Technologies) was duplexed with an equal concentration of Alt-R® CRISPR-Cas9 tracrRNA (Integrated DNA Technologies #1072532) in duplex buffer (IDT #1072570). An injection mix consisting

Table 1 sgRNA sequences used for transgenic strain construction

sgRNA name	Sequence
<i>dpy-10</i> sgRNA	GCUACCAUAGGCACCAGGAG
<i>syp-2</i> guide 1 sgRNA	AUUUAUAACUUGUCAGCCCA
<i>syp-2</i> guide 2 sgRNA	UUACGACAAACUUCUGGAUU
<i>syp-2</i> guide 3 sgRNA	ACAAGAUCUGACAAUGGAGC
<i>syp-2</i> guide 4 sgRNA	AAUGACACAAGAUCUGACAA

syp-2 guide 1 and 2 were used together in the same injection mix to generate ck38 and *syp-2* guide 3 and 4 were used together in the same injection mix to generate line ck39.

of 0.5 μM of each sgRNA duplex mix, 0.31 μM of Cas9 Nuclease V3 (IDT #1081058), 0.5 μM of *dpy-10* sgRNA, 0.5 μM of *dpy-10* ssDNA Oligo HDR template for positive selection (Table 2), and 0.115 μM of amplified and purified SYP-2::GFP gBlock (for generation of ck38 strain) (Table 2) or 5 μM of Oligo HDR Syp2(AMTA) ssDNA template (for ck39 allele) (Table 2) was made and injected into young adult N2 animals. The ck39 allele was made by injecting the corresponding injection mix targeting the mutation site into young adult ck38 animals. Both created strains were sequence verified and outcrossed to N2 5 times before phenotypic analysis.

Immunofluorescence

Measurements of aggregate frequency at different temperatures was performed using live imaging of *syp-2(ok307) V*; *wglIs227* in the GFP channel at 48 h after L4 stage, after being grown from larval stage L4 at 16°C or 20°C, or after being after growth at 20°C and then shifted to 25°C for 24 h.

Immunofluorescence was performed as previously described (ref, in press). Primary antibodies used in this study: goat anti-SYP-1 (Harper et al. 2011) (1:1500), chicken anti-GFP (1:300) (Aves Labs GFP-1020), rabbit anti-SYP-2 (1:500) (a kind gift from Sarit Smolikove, U. Iowa). The following secondary antibodies were used: donkey anti-goat Alexa Fluor 488 (1:500; Invitrogen A11055), donkey anti-rabbit Alexafluor 488 and 594 (1:500; Thermofisher A-21206 and A-20217, respectively) and donkey anti-chicken Alexa Fluor 594 (1:1000; Jackson Immuno Research Laboratories 703-586-155).

RNA interference

Plasmids were transformed into HT115 cells, and grown in culture overnight for 12–15 h with 100 μg/ml ampicillin, followed by an induction step with 1 mM IPTG for 2 additional hours before plating on 100 μg/ml ampicillin-1 mM IPTG NGM plates and grown at 25°C for 2 days. Synchronized L1s were added to RNAi plates and grown to 24 h past larval L4 stage at 20°C before being shifted to 25°C for 24 h before analysis. Knockdown of *dlc-1* was achieved by cloning a 700 base pair *dlc-1* genomic segment (see Table 3 for primer pairs) into the L4440 vector multi-cloning site. Knockdown of *htp-3* was achieved using Source Bioscience clone F57C9.5 (Kamath et al. 2003). Empty vector control RNAi was performed using the L4440 parent plasmid.

Hexanediol treatment

1,6-hexanediol treatments performed essentially as described previously (Rog et al. 2017). Live animals were dissected on poly L-lysine coated slides in 1x egg buffer + 2.5 mg/ml levamisole to immobilize animals. Slides were imaged immediately, and then 2x volume of 10% 1,6-hexanediol (dissolved in 1x egg buffer) was gently added underneath the coverslip, images were taken at 30 s and again 1 min after addition of 1,6-hexanediol. Gonads that

Table 2 Repair templates used for transgenic strain construction

Name	Oligo HDR repair template sequence 5' to 3'
<i>dpy-10</i> ssDNA	CACTTGAACCTCAATACGGCAAGATGAGAATGACTGGAAACCGTACCGCaTgCGGTGCCTATGGTAGCGGAGCTT-CACATGGCTTCAGACCAACAGCCTAT
<i>syp-2::gfp</i> gBlock®	CAATGATGTTTCAGGCGGCTATAAAAAATAATCAATAATGCAAAAATCAACAACGATGGGTCTCAGGAAGATTTCT-CTGCTCATTACGACAAACTTCTGGATCTCGTTGAAACGCTCGAGCCGTGGGCTGACAAGTTA GGAGGTGGAGG-TGGAGCT ATGAGTAAAGGAGAAGAACTTTTCACTGGAGTTGTCCCAATCTTGTGAATTAGATGGTGATGTT-AATGGGCACAAAATTTTCTGTCAGTGGAGAGGGTGAGGGTGATGCAACATACGGAAAACTTACCCTTAAATTTA-TTTGCACTACTGGAAAACCTACCTGTTCCATGGGTAAGTTTAAACATATATACTAACTAACCCCTGATTATTT-AAATTTTCAGCCAACACTTGTCACTACTTTCTGTTATGGTGTTCATGCTTCTCGAGATACCCAGATCATATGA-AACAGCATGACTTTTTCAAGAGTGCCATGCCCGAAGGTTATGTACAGGAAAGAATATATTTTCAAAGATGA-CGGGAACTACAAGACACGTAAGTTTAAACAGTTCGGTACTAACTAACCATACATATTTAAATTTTCAGGTGCT-GAAGTCAAGTTTGAAGGTGATACCCTTGTAAATAGAATCGAGTTAAAAGGTATTGATTTTAAAGAAGATGGAA-ACATTCTTGGACACAAAATTGGAATACAATACTATACTACACAATGTATACATCATGGCGGACAAAACAAAAGAA-TGGAAATCAAAGTTGTAAGTTTAAACATGATTTTACTAACTAACTAATCTGATTTAAATTTTCAGAACTTCAA-ATTAGACACAACATTGAAGATGGAAGCGTTCAACTAGCAGACCATTATCAACAAAATACTCCAATTGGCGATG-GCCCTGTCTTTTACCAGACAACCATTACCTGTCCACACAATCTGCCCTTCGAAAGATCCCAACGAAAAGAG-AGACCACATGGTCTTCTTGAGTTTGTAAACAGCTGCTGGGATTACACATGGCATGGATGAACTATACAAAataaa-tcatctgttgattcaattcctgtttattacatgacatgacatcatttaattgttgcctatgcatgattgcttctcaaatatggg
<i>syp-2</i> (AMTA) ssDNA	GGATGACGTTTCTGAAATTTGAACACAAAATGATCAAGCAGGCGctatgacagctGATCTGACAATGGAGCTCGCAA-ATTCAATCGAACGTATCGCAAATATGGCATTAGC

Underlined, lowercase sequence indicates nonsilent mutations. Uppercase, underlined letters indicate silent mutations to PAM sites. Bold letters indicate GGGGGA linker sequence and uppercase letters following bold letters indicate *gfp* sequence. PAM site mutation for *syp-2::gfp* (AMTA) strain was not integrated into the genome as confirmed with strain sequencing.

Table 3 Primers used to amplify regions of genes from genomic DNA to insert into L4440

Gene	Forward primer	Reverse primer
<i>dlc-1</i>	GGTACCACG TAGGATCAGGTCACAA	GGGGCCG CCGCATCACAACCGTTATT

Blue letters represent added restriction sequences (NotI and KpnI) for ease of addition into the multi-cloning site of the L4440 vector.

were fixed and probed with antibodies were treated with 1x volume of 10% 1,6-hexanediol for 1 min before fixation.

Brood assays

Larval stage L4 animals were singled out and grown at the temperature specified, moving animals to fresh plates every 20–25 h until the animal ceased producing embryos for 24 h. Twenty-four hour after removal of the adult, plates were scored for number of remaining unhatched embryos. Males and hermaphrodite progeny were counted at young adult stage. Each temperature for each strain had 9–12 replicates.

Western blot analysis

Protein extraction and western blots were performed as previously described (Nadarajan et al. 2016), with some modifications. Modifications include using 20 synchronized, confluent 10 cm plates of young adult animals grown at 25°C for each strain, and after freezing samples in liquid nitrogen, a 1.5x lysis buffer [75 mM Hepes pH 7.5, 1.5 mM MgCl₂, 150 mM KCl, 0.1% NP-40, and 15% glycerol, with complete EDTA free protease inhibitor cocktail (Roche 11836170001)] was used for lysing and freezing samples. To lyse animals, samples were sonicated for 15 s on, 45 s off for 18–25 min, followed by addition of 2x SDS Sample Buffer and heated at 95°C for 5 min.

Fifty micrograms of total protein from each sample was loaded onto a precast 4–12% gradient Bis-Tris gel (Invitrogen NW04120BOX) and transferred onto a PVDF membrane using a Power Blotter (ThermoScientific 22834SPCL). Blots were blocked with 5% Bovine Serum Albumin in TBS + 0.1% Tween-20 (TBS-T) for 2–3 h before incubation with primary antibody at 4°C overnight. After three 10 min washes with TBS-T, blots were incubated with secondary antibodies for 3 h at room temperature, followed by the same wash procedure. Blots were incubated with Clarity Western ECL substrate (BioRad 170-5060) for five minutes

and visualized using the Bio-Rad ChemiDoc Imaging System and signal was quantified using ImageJ. Primary antibodies used were chicken anti-GFP (1:2000) (Aves Labs GFP-1010), mouse anti-actin (1:2000) (Chemicon MAB150). Secondary antibodies used were donkey anti-chicken HRP (1:2000) (Jackson #703-035-155), donkey anti-mouse HRP (1:2000) (Jackson 715-035-151).

Statistical analysis

All brood size data (total brood size, % dead embryos, and % males) were tested for normal distribution using the Kolmogorov–Smirnov Test for Normality, and all except % males in N2 grown at 16°C and 25°C were not significantly different from a normal distribution, which is expected as spontaneous male generation is a very infrequent event. Brood size, embryonic lethality, and % male progeny were compared using one-way ANOVA followed by Tukey's *post hoc* multiple comparison tests. DAPI body frequency was tested by using a chi-squared goodness of fit for the categories of DAPI bodies 6–8, using the proportions from the *syp-2::gfp* WT, or *syp-2::gfp* WT; *dlc-1::flag*; *dlc-1* as the expected ratios.

Results

Knockout of dynein heavy chain and/or dynactin does not induce SYP foci formation

Previous reports indicated that RNAi-mediated knockdown of *C. elegans dlc-1* in combination with dynein heavy chain (*dhc-1*) temperature sensitive (*ts*) mutants raised at 25°C results in the formation of SYP protein foci not associated with chromatin in hermaphrodite meiosis (Sato et al. 2009). However, in similar experiments we found that raising *dhc-1* (*or195^{ts}*) mutants alone at the restrictive temperature (25°C) without *dlc-1* (RNAi) did not typically result in the SYP protein foci phenotype (Figure 1). In these experiments, we did observe other expected *dhc-1* mutant

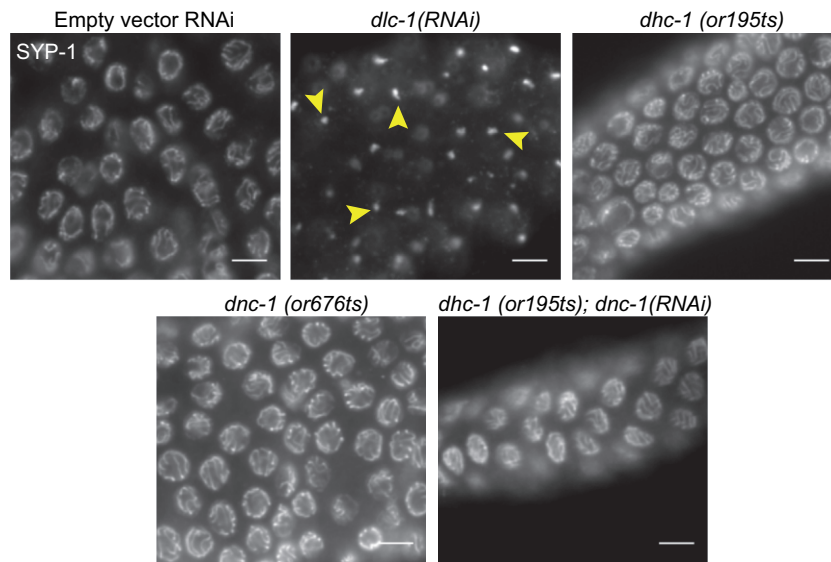


Figure 1 DLC-1 but not other dynein complex components are required for CE protein loading. Animals were raised at 25°C for 24 h before gonads were dissected, and whole mount fixed and probed with anti-SYP-1. All RNAi-treated animals were N2 animals raised on RNAi from larval stage L1. Images show early pachytene region of ovary. Top left: WT N2 gonad treated with empty vector control RNAi for comparison. Top middle: *dlc-1(RNAi)* animals display foci of SYP-1 in each nucleus (arrowheads), while both temperature sensitive mutants of *dhc-1(or195ts)* (top right) and *dnc-1(or676ts)* (bottom left) display normal synapsis. RNAi knockdown of *dnc-1* in a *dhc-1(or195ts)* mutants yields normal synapsis of chromosomes (bottom right). Meiotic progression is depicted from left to right. Scale bars 5 μ m.

phenotypes, including embryonic lethality and polyploid nuclei in the mitotic region of the gonad (not shown). A temperature-sensitive mutant of another component of the dynein complex, *dnc-1(or676)*, also did not display SYP foci in mutants raised at the restrictive temperature, despite also displaying embryonic lethality. Furthermore, *dnc-1(RNAi)* combined with *dhc-1(or195^{ts})* worms also did not display SYP foci when raised at the restrictive temperature (Figure 1). In contrast, as has been previously reported, RNAi-mediated knockdown of DLC-1 alone in WT N2 animals raised at 25°C resulted in formation of the SYP foci (Bohr et al. 2015) (Figures 1 and 2, and discussed further below). These results indicate that the requirement for DLC-1 in meiotic progression and synapsis may be independent of its role in dynein motor activities.

SYP proteins form foci in a temperature sensitive manner with knockdown of DLC-1

While performing RNAi knockdown of DLC-1, we observed temperature-dependent differences in frequency of the SYP foci phenotype. When grown at 20°C, 61% of gonads have SYP-2 foci, while growth at 25°C results in 85.88% of gonads having SYP-2 foci (Figure 2, A and C). Interestingly, when grown at 16°C, 0% of *dlc-1(RNAi)* gonads display the SYP foci phenotype (Figure 2, A and C). In contrast, *htp-3(RNAi)* animals grown in parallel resulted in SYP-2 foci in 100% of gonads at all three temperatures, indicating that these results are unlikely to be due to temperature-dependent differences in RNAi efficiency of meiotic targets. In addition, the higher the growth temperature the more severe the phenotype of *dlc-1* knockdown observed: *dlc-1(RNAi)* animals grown at 25°C typically displayed longer regions of nuclei with SYP-2 foci (Figure 2A), and regions without SYP-2 foci appeared to have more diffuse SYP-2::GFP localization than *dlc-1(RNAi)* animals raised at 20°C (Figure 2B). This diffuse localization of SYP-2::GFP in nuclei without foci could indicate increased inability to form normal SC structures at 25°C, could be an intermediate before foci formation, or could indicate lower levels of protein or a lower amount of SC assembly onto chromatin. In any of these

cases, this suggests a more severe phenotype of *dlc-1(RNAi)* at 25°C of affected gonads, even in nuclei that do not display the foci phenotype. In addition, in *dlc-1* animals grown at 25°C, SYP-1 and SYP-2::GFP co-localize, indicating that additional SYP proteins coalesce into the foci, and that there is no cleavage of SYP-2::GFP in the *wgIs227; syp-2(ok307)* strain, even at elevated temperatures (Supplementary Figure S1).

SYPs form insoluble foci with knockdown of DLC-1

CE protein “polycomplexes” are often observed as normally transient foci in pre-meiotic nuclei that precede SYP protein loading into a more stable SC (Goldstein 2013; Rog and Dernburg 2015). In the absence or disruption of axial elements, such as in *htp-3* mutants, these polycomplexes are stabilized and remain unassociated with chromatin for the rest of meiosis (Goodyer et al. 2008). Similar to the normal SC that assembles onto chromosomes, polycomplexes are reversibly dissolved by amphiphilic solvents such as 1,6-hexanediol (Rog et al. 2017). In contrast to polycomplexes, CE aggregates formed at elevated temperatures above 26.5°C are resistant to dissolution (Rog et al. 2017). We confirmed that foci caused by *htp-3(RNAi)* were dispersed by 1,6-hexanediol in 100% of the gonads examined (Figure 3, Supplementary Figure S2). Heat-induced foci were less susceptible to 1,6-hexanediol, although some dispersal was observed. In our hands, adding 1,6-hexanediol caused dispersal of foci in 59.4% of gonads in *syp-2::gfp(wgIs227)* animals raised at 27°C, and 22.9% of *syp-3::gfp(ok758; ieSi11)* animals raised at 27.5°C (Supplementary Figure S3). In contrast, 100% of SYP-2 foci in *dlc-1(RNAi)* animals grown at 25°C were resistant to 1,6-hexanediol treatment, and thus are even less soluble than the heat induced aggregates (Figure 3, Supplementary Figure S2). This indicates that there is a difference in the way the SYP foci form after *dlc-1(RNAi)* knockdown at 25°C as compared to both normal SC assembly and polycomplex assembly in the absence of HTP-3. We further verified that SYP-1 and SYP-2::GFP co-localized in foci induced by all conditions examined: *htp-3(RNAi)* animals, *dlc-1(RNAi)* animals, and in animals raised at 27.5°C (Supplementary Figure S1). Thus both

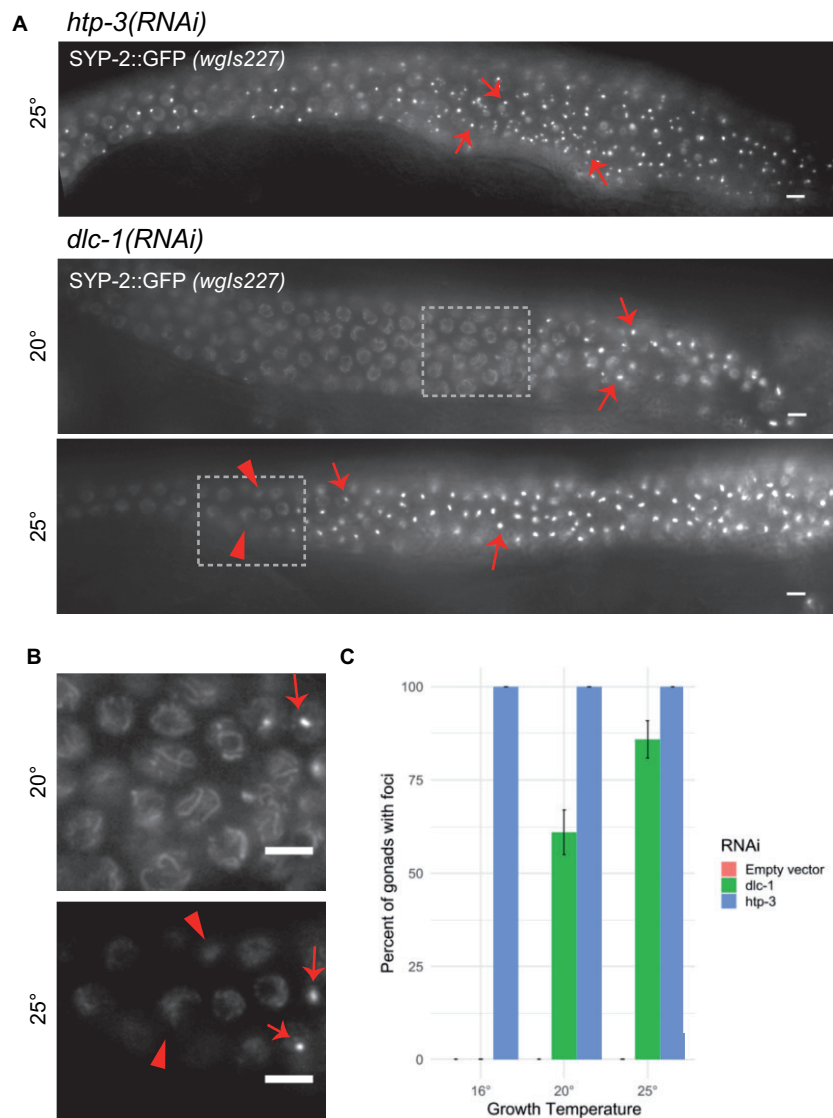


Figure 2 Synapsis defect in *dlc-1(RNAi)* is temperature sensitive. (A) Live GFP visualization of SYP-2::EGFP in *wglIs227; syp-2(ok307)* V animals raised on *dlc-1* or *htp-3* dsRNA from larval stage L1, and analyzed at 48 h post-larval L4 stage. *htp-3(RNAi)* animals always display SYP-2::GFP foci. *dlc-1(RNAi)* animals raised at both temperatures display foci of SYP-2::GFP (arrows). Boxed portions of (A) shown at higher magnification in (B). Unaffected nuclei display normal SYP-2 loading in *dlc-1(RNAi)* at 20°C, but show less structured localization in *dlc-1(RNAi)* at 25°C in nuclei preceding foci formation (arrowheads). (C) Percentage of gonads with extended regions of SYP foci in *dlc-1(RNAi)* animals. The SYP foci phenotype is not temperature sensitive in *htp-3(RNAi)* animals in which 100% of gonads display the phenotype at all temperatures assayed ($n > 60$ total gonads scored at each temperature). Animals fed empty vector control never displayed the SYP foci phenotype at any of the three temperatures measured ($n > 60$ total gonads scored at each temperature). Meiotic progression displayed from left to right in all images. Scale bars 5 μ m.

SYP-1 and SYP-2 interact in SYP foci irrespective of the conditions causing them.

Evidence of SYP-2/DLC-1 interactions

Dynein light chains in other organisms have been reported to interact with many different proteins via two consensus binding motifs (Lo et al. 2001). These binding motifs are frequently found next to a coiled-coil domain in the target protein (Rapali et al. 2011). We examined the protein sequences of axial and CEs of the *C. elegans* SC and identified a potential binding motif (96-KMTQ-99) located next to a predicted coiled-coil domain (98-161) of SYP-2 (Figure 4A) (Schild-Prufert et al. 2011). Interestingly, whereas the structure of CE proteins is conserved between organisms, the sequences of CE proteins are not well conserved (Page and Hawley 2001; MacQueen et al. 2002). However, one CE protein in both humans and yeast contains a potential DLC-1 binding motif

located next to a coiled-coil domain, implying that this motif may be important for the function of those CE proteins (Figure 4A).

To examine the importance of the putative DLC-1 interaction domain, we first used CRISPR-Cas9 to tag the endogenous SYP-2 with GFP [*syp-2(ck38)*, hereafter denoted as “WT *syp-2::gfp*”]. This “WT” SYP-2::GFP exhibits a distribution and SC pattern indistinguishable from the endogenous, untagged SYP-2 (Supplementary Figure S4). We note, however, that this strain exhibits a slight increase in some phenotypes, indicating that the GFP tag causes subtle defects in some aspect of normal SYP-2 function (e.g., Figure 5). We further used CRISPR-Cas9 to mutate the putative binding sequence in *syp-2::gfp* from 96-KMTQ to 96-AMTA [*syp-2(ck39)*, hereafter denoted as *syp-2::gfp(AMTA)*]. The SYP-2::GFP(AMTA) localization to chromatin was generally similar to WT protein, except where noted below and no difference between SYP-2 protein localization and that of GFP in these strains was

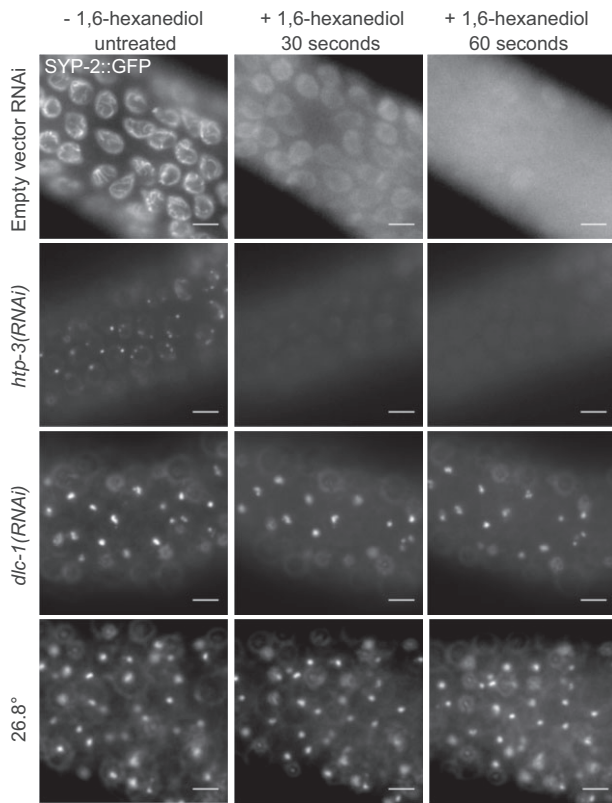


Figure 3 SYP foci formed with DLC-1 reduction or exposure to elevated temperature are resistant to hexanediol. Live GFP visualization in age-matched *wgIs227; syp-2(ok307)* gonads treated with either empty vector control, *htp-3*, or *dlc-1* dsRNA, or grown at a restrictive temperatures, with images taken immediately before exposure to 6.67% 1,6-hexanediol (first column), then 30 s (second column) and 60 s (third column) after exposure. The SC in animals fed control dsRNA (top row), and SYP-2: GFP foci in *htp-3(RNAi)* (second row) animals dissipate after addition of hexanediol. In contrast, *dlc-1(RNAi)* animals display persistent SYP foci after the addition of hexanediol (third row), similar to SYP foci formed in animals grown at 26.8°C for 24 h (bottom row). Scale bars 5 μ m.

observed (Supplementary Figure S4). Typically there is a short region where transient SYP polycomplexes are observed in a few pre-meiotic nuclei (Goldstein 2013; Rog and Dernburg 2015). In *syp-2::gfp(AMTA)* gonads, we observed a slight but significant lengthening of this region when animals were raised at 20°C as compared to WT *syp-2::gfp* animals (Figure 4, B–D). In addition, mutant *syp-2::gfp(AMTA)* animals raised at all temperatures displayed more proximal nuclei with chromosomes clustered together at the nuclear periphery, reminiscent of transition zone nuclei, which are normally still in the process of pairing homologous chromosomes and initiating synapsis (Supplementary Figure S5).

The addition of GFP to endogenous SYP-2 had little effect on brood size compared to N2 at all three temperatures measured (Figure 5A). In contrast, the *syp-2::gfp(AMTA)* animals exhibited a significantly decreased brood size at all temperatures compared to both N2 and WT *syp-2::gfp* (Figure 5A). The *syp-2::gfp(AMTA)* strain's brood also exhibited a significant rise in embryonic lethality at all three temperatures, but dramatically increased embryonic lethality at 25°C (64% of embryos failed to hatch; Figure 5B). The increase in embryonic lethality was accompanied by an increase in XO males in the surviving offspring at all temperatures (Figure 5C), an indication of defects in homolog pairing, synapsis, and/or X chromosome nondisjunction (Hodgkin et al. 1979). This also suggests that the increased embryonic lethality

was due to increased aneuploidy in the offspring, which was confirmed by an observable increase in the appearance of achiatic univalents in oocytes (Supplementary Figure S6). Addition of the GFP tag to WT SYP-2 did cause a slight but significant increase in the incidence of males among surviving progeny, but at a significantly lower level than AMTA SYP-2 (Figure 5).

Although the SC incorporation pattern of the AMTA mutant in meiotic nuclei was not observably different than that of the WT SYP-2::GFP after early meiosis, the fluorescence signal appeared to be less bright in the AMTA strain. We prepared equal total protein lysates from each strain and probed the level of each protein by western blot. Indeed, the SYP-2::GFP (AMTA) protein levels were reduced at 20°C at 25°C compared to the WT SYP-2::GFP grown at the same temperature (Figure 6). Multiple western blots from separate biological replicates confirmed a decrease in SYP-2::GFP (AMTA) abundance, although fluctuations in total SYP-2 signal at 20°C made the change at that temperature less significant (Figure 6B). Given that the AMTA mutation was created in the WT *syp-2::gfp* allele at the endogenous locus, we interpret this to be most likely caused by decreased protein stability caused by the KMTQ to AMTA mutations, although decreased mRNA production or stability cannot be ruled out.

We next tested for any interactions between SYP-2 and DLC-1 that might depend on the putative interaction domain. We crossed the *syp-2::gfp* alleles into a *dlc-1* deletion strain, *dlc-1(tm3153)*, carrying an integrated, single copy FLAG-tagged *dlc-1* transgene that rescues the *dlc-1(tm3153)* lethal phenotype (hereafter referred to as *dlc-1::flag* instead of *dlc-1::flag; dlc-1*) (Wang et al. 2016). We were unable to consistently detect DLC-1:FLAG interactions with either the WT SYP-2::GFP or the SYP-2::GFP(AMTA) using anti-GFP immunoprecipitations followed by anti-FLAG western blots (not shown). However, we noticed that the line carrying the *dlc-1::flag* transgene had an increase in embryonic lethality and males at 20°C and 25°C (Figure 7B). The presence of the *dlc-1::flag* transgene clearly had a substantial temperature dependent impact on meiosis when combined with the SYP-2 AMTA mutation, including increased embryonic lethality, and increased univalent formation (Figure 7, Supplementary Figure S6). We therefore assume that the high levels of embryonic lethality are due to increased aneuploidy in the offspring. In addition, the increase in embryonic lethality at 25°C in the SYP-2::GFP (AMTA) carrying the *dlc-1::flag* transgene compared to without was significant (ANOVA $P \leq 0.0001$; Tukey's test $P = 0.0017$), but the increase in males was not (Tukey's test $P = 0.2217$). We observed a high variability in frequency of males between broods, which likely prevents statistical significance, and is likely due to the stochastic survival of XO males among the high frequency of dead embryos. These results suggest that although the integrated *dlc-1::flag* transgene largely rescues the embryonic lethality of the *dlc-1(tm3153)* deletion, its rescue is incomplete and is hypomorphic. Strikingly, the majority of the *syp-2::gfp(AMTA); dlc-1::flag* animals, but not the WT *syp-2::gfp; dlc-1::FLAG* animals, also showed near complete aggregation of the SYP-2::GFP in their germ cells (Figure 7A). Interestingly, no SYP-2::GFP aggregates were observed in *syp-2::gfp(AMTA); dlc-1::flag* males (0/23 at 25°C), similar to the lack of such aggregates in *dlc-1(RNAi)* males (Supplementary Figure S7).

These results suggest a specific genetic interaction between the "hypomorphic" *dlc-1::flag* transgene and the *syp-2::gfp(AMTA)* allele carrying a mutation in a putative interaction domain. However, it should be noted that the addition of GFP to the AMTA mutant could conceivably also partially contribute to the observed phenotypes observed in the presence of the *dlc-1* transgene, as

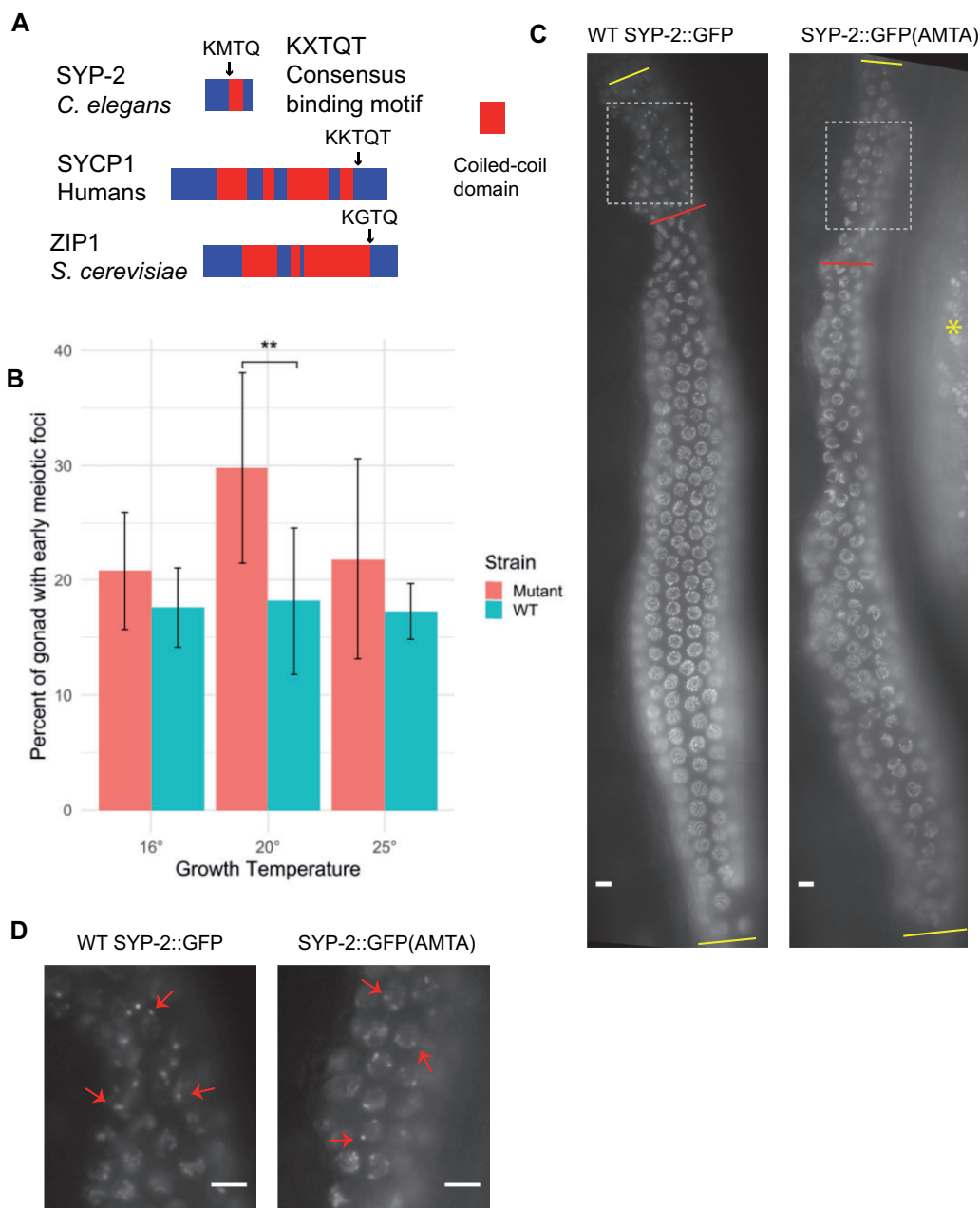


Figure 4 Mutation of a putative DLC-1 binding site in SYP-2 results in meiotic defects. (A) DLC-1 orthologs in other species interact with a consensus binding motif (KXTQT) in other proteins, normally located in close proximity to a coiled-coil domain. *C. elegans* SYP-2 protein contains a similar motif (black arrow) located next to its coiled-coil domain (red block). A similar potential binding motif adjacent to a coiled-coil domain is found in CE proteins in both human and yeast. (B) *syp-2::gfp(AMTA)* mutant gonads have a significantly larger % of their gonads that have SYP-2::GFP foci at 20°C than age matched WT *syp-2::gfp*. While *syp-2::gfp(AMTA)* gonads have larger percentages than WT at other temperatures, it is not significant. Eight to nine WT *syp-2::gfp* and 12-13 *syp-2::gfp(AMTA)* gonads were analyzed at each temperature. Statistical comparisons performed using Student's T test (** $P \leq 0.01$). (C) Live imaging of GFP in WT *syp-2::gfp* hermaphrodite and in *syp-2::gfp(AMTA)* hermaphrodite grown at 25°C. Zone with foci were measured (from first yellow bar to red bar), and divided by total length of meiotic region (between yellow bars) to give data in B. In the *syp-2::gfp(AMTA)* image, there is autofluorescence from the gut on the right (red asterisk). Gray boxes indicate regions magnified in D. (D) Magnified early meiotic SYP-2 foci (arrows) in both WT *syp-2::gfp* and *syp-2::gfp(AMTA)*. Meiotic progression from top to bottom in all images. Scale bars 5 μ m.

syp-2::gfp; dlc-1::flag animals have a slight increase in males at 25°C as compared to the *dlc-1::flag* animals alone (Figure 7B).

Discussion

DLC-1 may work as a protein chaperone for SYP proteins at high temperatures

We found that although it is reported to play an important role in chromosome movement during homolog pairing, disruption of

the dynein motor complex does not appear to affect the subsequent ability of the SC to form and synapsis to occur between chromosomes. Instead, specific loss of just the DLC-1 results in the formation of insoluble SYP protein aggregates. Defects in or knockdown of multiple other dynein complex components, alone or in combination, did not appear to dramatically affect SC assembly between chromosomes. Thus, there is a dynein motor independent function for DLC-1 that is normally required to prevent improper aggregation of SYP proteins and help guide

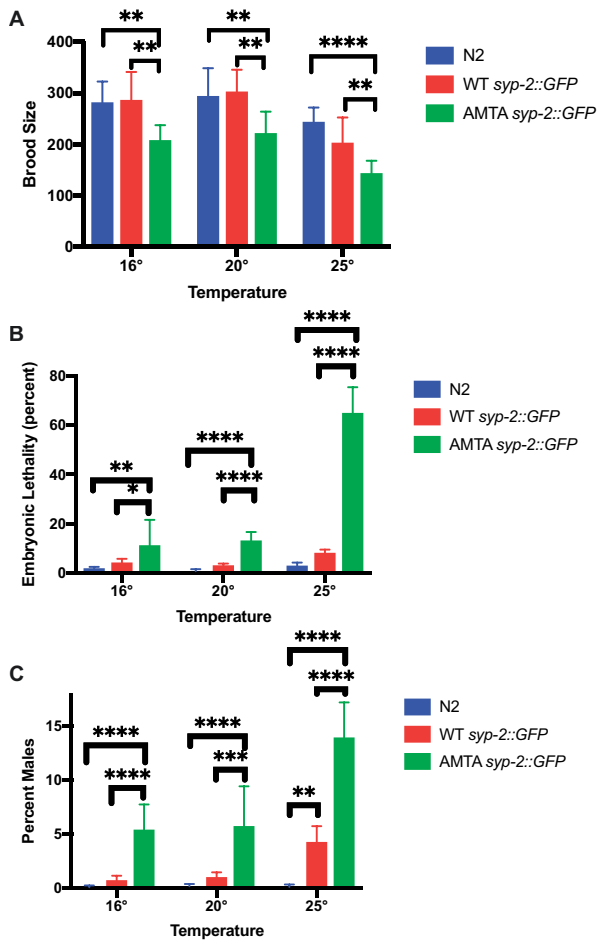


Figure 5 Mutation of the putative DLC-1 binding site in SYP-2 causes temperature-sensitive embryonic lethality and meiotic defects. 9–12 WT *syp-2::gfp*, +/+ (strain N2), or AMTA *syp-2::gfp* animals were singled out for each temperature and their progeny statistics were recorded. (A) Brood size analysis. All embryos were counted until the animal no longer laid embryos for 24 h. At all temperatures, the (AMTA) *syp-2::gfp* mutation had a significantly lower brood size than both WT *syp-2::gfp* and +/+. (B) Embryonic Lethality: Unhatched embryos were counted 24 h after the adult was moved to the next plate and % unhatched were graphed. The (AMTA) *syp-2::gfp* mutation has a significantly higher embryonic lethality than +/+ at all temperatures, and the embryonic lethality significantly increases at 25°C, with 64% of embryos failing to hatch. (C) Percent of the living brood that were male. At all temperatures, the (AMTA) *syp-2::gfp* mutation has a significantly higher rate of males than both WT *syp-2::gfp* and +/+, with the amount of males at 25°C significantly higher than both other temperatures ($P < 0.0001$). One +/+ animal grown at 16°C was excluded from all analyses as it had an outlying brood size of 61. ANOVA followed by Tukey's *post hoc* test was used for statistical analysis. * $P \leq 0.05$, ** $P \leq 0.01$, *** $P \leq 0.001$, **** $P \leq 0.0001$.

normal SC assembly onto chromatin. This function is temperature dependent, as foci formation upon loss of DLC-1 increases with increasing temperatures, with ~80% of ovaries exhibiting SYP aggregates at 25°C.

SYP proteins that are properly assembled into an interhomolog SC have hydrophobic interactions that can be reversibly disrupted by 1,6-hexandiol, as can SYP protein polycomplexes that spontaneously form when there is no lateral axis available for assembly (e.g., *htp-3* mutants or *htp-3(RNAi)*) (Rog et al. 2017). In contrast, foci formed in *dlc-1(RNAi)* animals are no longer disrupted by the amphiphilic solvent, implying that the foci that result from DLC-1 knockdown are not structurally similar to previously

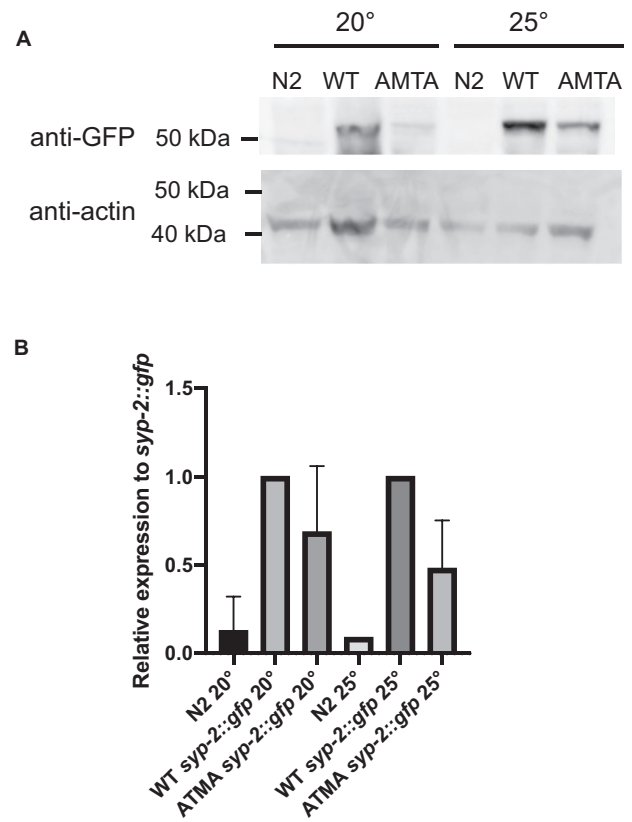


Figure 6 Decreased Abundance of AMTA Mutant SYP-2 Protein. (A) Fifty micrograms of protein prepared from N2, WT *syp-2::gfp*, and AMTA *syp-2::gfp* animals grown at 20°C or 25°C, run on acrylamide gel, transferred to western blot and probed with anti-GFP (top) or anti-actin (bottom). (B) Band intensity quantified using ImageJ of two biological replicates, with anti-GFP signal intensity normalized to actin of corresponding sample, then further normalized to *syp-2::gfp* sample grown at the same temperature. GFP is expressed at a lower level in *syp-2::gfp*(AMTA) animals than in *syp-2::gfp* animals at both temperatures, although less significantly so at 20°C.

described polycomplexes. Instead, the temperature-dependent foci produced by loss of DLC-1 are more reminiscent of the aggregates that occur when animals are grown at temperatures above 26.5°C (Rog et al. 2017). It was proposed that these heat-induced aggregates result from a change of protein structure into a partially denatured state (Rog et al. 2017). We hypothesize that the aggregates that are induced by DLC-1 depletion at 20°C and 25°C are similarly the result of a change in protein structure that is normally prevented by DLC-1's association with SYP-2 and possibly other components. We further hypothesize that the temperature-sensitive requirement for DLC-1 to prevent SYP aggregation is due to its role as a type of chaperone required to guide SYP protein assembly in the earliest stages of meiosis, a role that is increasingly essential as temperatures increase.

In early meiotic stages, there are small SYP protein foci that are likely transient polycomplexes that normally and dynamically form as SYP protein synthesis initiates in pre-meiotic cells. As these proteins are prone to self-assembly, a mechanism likely exists to help prevent stable polycomplex and/or insoluble aggregate formation of newly synthesized SYP proteins as axis formation and pairing requirements delay SC assembly on chromatin. Our results support a role for DLC-1 in this stabilization process: in the absence of DLC-1, irreversible aggregation is favored over polycomplex formation as temperatures rise (Figure 8). This is in

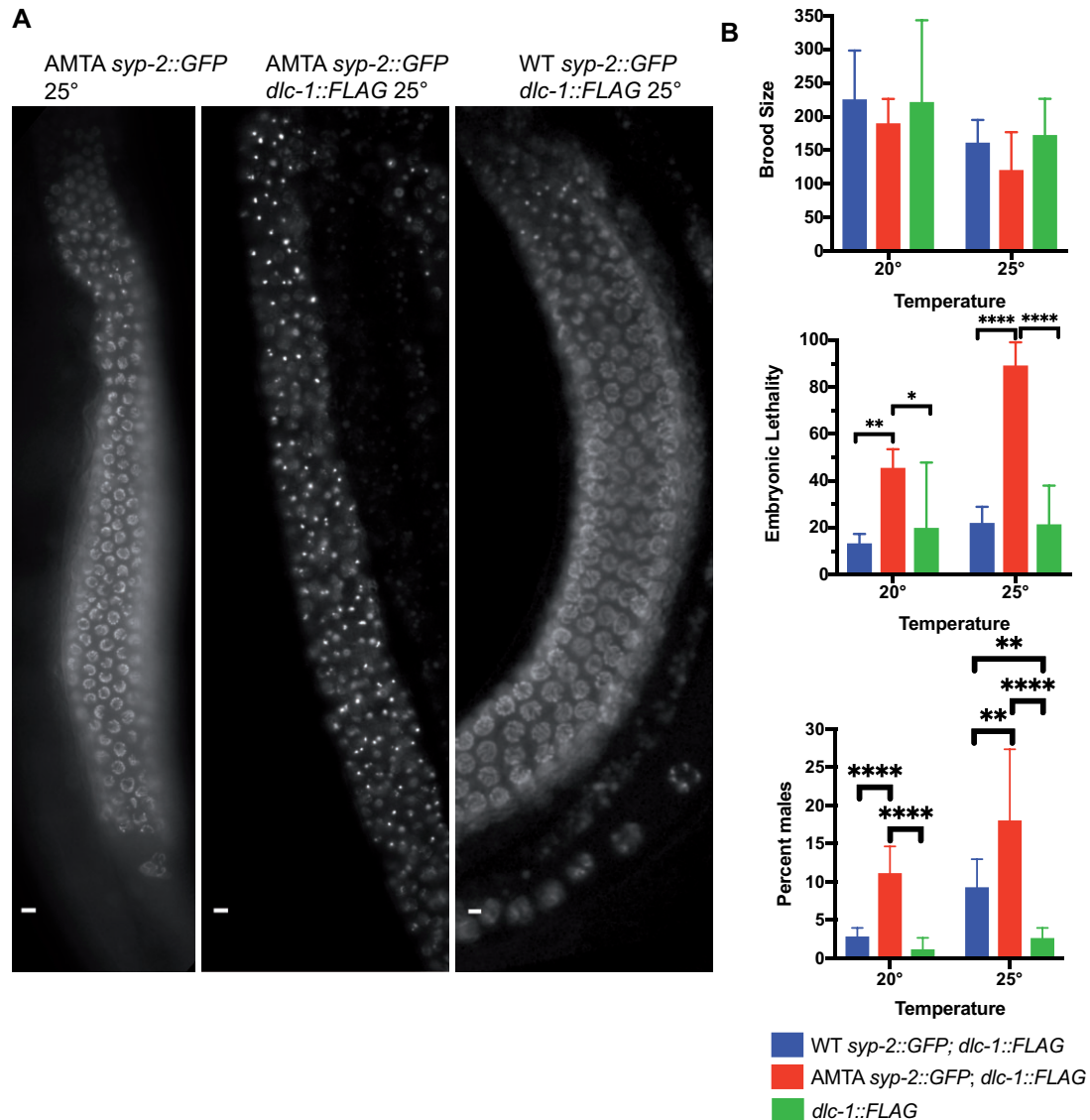


Figure 7 DLC-1::FLAG transgene enhances AMTA mutant defects. (A) Live imaging of GFP in AMTA *syp-2::gfp*, WT *syp-2::gfp*; *dlc-1::flag*, and AMTA *syp-2::gfp*; *dlc-1::flag* animals grown at 25°C. Flag tagging DLC-1 in the AMTA strain results in SYP aggregates seen in *dlc-1(RNAi)* animals. (B) 8–15 WT *syp-2::gfp*; *dlc-1::flag*, AMTA *syp-2::gfp*; *dlc-1::flag*, and *dlc-1::flag* animals were singled out for each temperature and progeny stats were recorded until each worm stopped laying embryos similar to Figure 5. The addition of the *dlc-1::flag* transgene increased embryonic lethality of the WT *syp-2::gfp* animals to 12.81% at 20°C and 21.5% at 25°C, while increasing embryonic lethality of AMTA *syp-2::gfp* animals to 44.98% at 20°C and to 88.66% at 25°C. ANOVA followed by Tukey's *post hoc* test was used for statistical analysis. * $P \leq 0.05$, ** $P \leq 0.01$, *** $P \leq 0.001$, **** $P \leq 0.0001$.

line with numerous reports that have shown dynein light chain homologs acting as protein chaperones guiding protein–protein interactions, in addition to the canonical role of the light chain in stabilizing folding and alpha-helix content of dynein intermediate chains during assembly of the dynein motor complex [reviewed in Rapali et al. (2011)].

It has previously been shown that using the AID system, degrading DHC-1 results in SYP foci (Zhang et al. 2015). However, we noticed that both these foci, and *htp-3(RNAi)* induced poly-complexes all result in multiple, small foci in each nucleus, which may indicate they are more like the small SYP foci that normally appear in pre-meiotic nuclei, whereas *dlc-1(RNAi)* induced aggregates tend to be large, with one to two per nucleus. The DHC-1 degradation-induced foci may be the result of a delay in early meiosis resulting from delayed homolog pairing (Wynne et al. 2012; Rog and Dernburg 2015). Our results do not rule out

the proposed role for dynein motors in homolog pairing, only that DLC-1 has a separate, presumably additional role in SC assembly.

The putative DLC-1 binding motif in SYP-2 is important, but not essential for SC function

We identified a potential DLC-1 interaction motif in SYP-2 and mutated it using CRISPR-directed mutagenesis. Mutation of the putative binding motif in SYP-2 with just two amino acid substitutions results in increased meiotic defects at 25°C. Synapsis still occurs despite the mutations, indicating that this motif is not absolutely essential for the function of SYP-2. However, when combined with a *dlc-1* transgene that rescues embryonic lethality caused by a *dlc-1* deletion, but does not completely rescue all DLC-1 function, meiosis is almost completely and irreversibly disrupted in most animals. This further indicates a genetic interaction between SYP-2 and DLC-1. The absence of this effect in

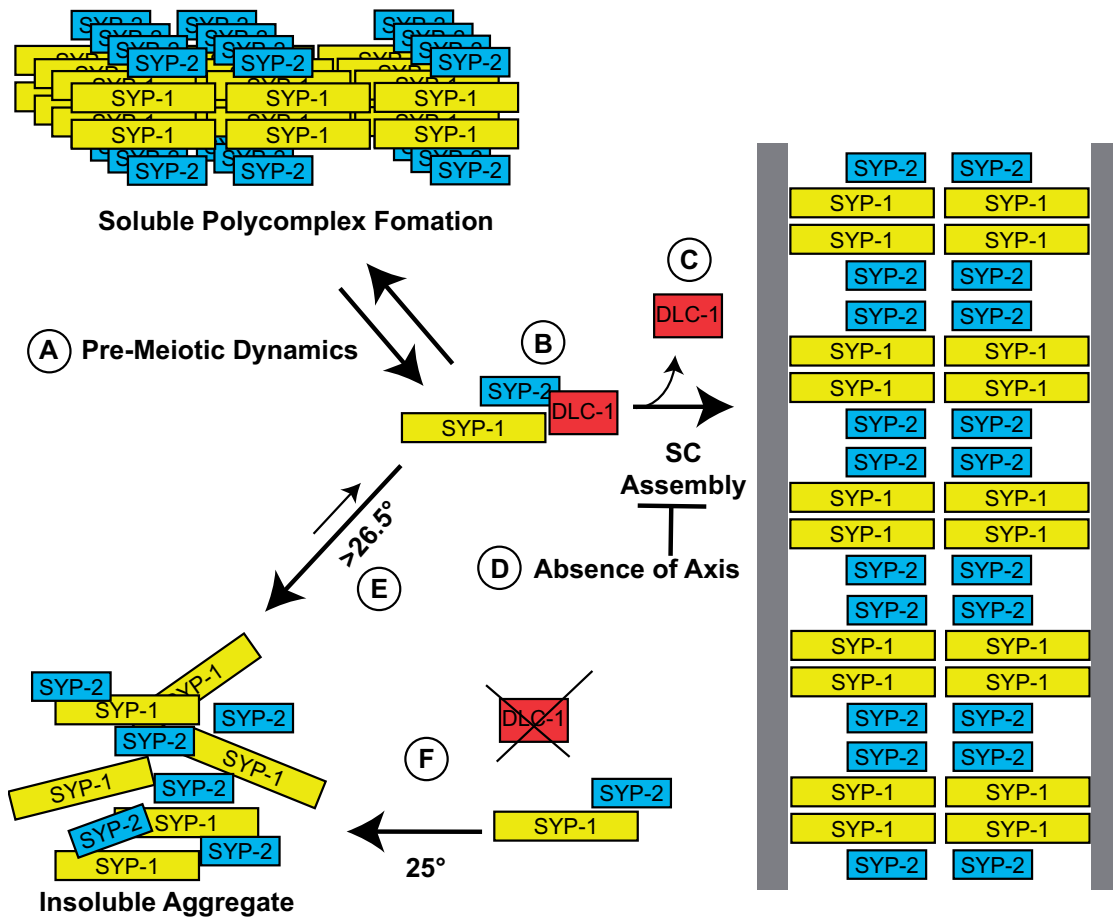


Figure 8 Model of DLC-1's role in pre-synapsis meiosis. (A) As meiosis begins, SYP proteins initially form small dynamic polycomplexes before the SC assembles onto paired homologs. (B) DLC-1 binding to SYP-2 helps to prevent temperature-dependent aggregation before synapsis initiates, (C) and disassociates during synapsis. (D) In the absence of axial components, assembly onto chromosomes is prevented, and polycomplexes are stabilized. (E) At temperatures higher than 26.5°C, SYP proteins no longer fold correctly and form insoluble aggregates away from chromosomes even in the presence of DLC-1. (F) Without DLC-1, and more frequently at temperatures approaching 25°C, SYP proteins will no longer fold correctly and also form aggregates away from chromatin.

males, which do not appear to require DLC-1 function in meiosis, suggests this is a specific effect involving a disrupted interaction between SYP-2 and DLC-1.

Dynein light chain, and even specifically *C. elegans* DLC-1, has been shown to bind to proteins without a canonical binding motif and can even bind to multiple sites within the same protein (Dorsett and Schedl 2009; Wang et al. 2016). The potential DLC-1 interaction motif we identified clearly has some impact on SYP-2's meiotic function and possibly protein stability, but does not appear to be the sole interaction component. Although its disruption has a minor effect on meiosis and SYP-2 stability, a major effect is revealed when paired with the *dlc-1* transgene. It is also possible that the severe phenotypes when the AMTA mutation is paired with the *dlc-1* transgene are an additive effect of multiple, partially disrupted interactions involving other SC components in addition to SYP-2.

Regardless, changing just two amino acids in the motif (KMTQ→AMTA) causes significant meiotic defects with some temperature dependence in these phenotypes. The AMTA mutant SYP-2 protein appears to be less stable than wild type at 25°C, and *syp-2(AMTA)* animals have a reduced brood size, high embryonic lethality at 25°C, and the progeny have a greatly increased incidence of males. All of these phenotypes are

exacerbated when the mutant protein is expressed in animals expressing what we propose to be a hypomorphic *dlc-1* transgene. The increase in X chromosome segregation abnormalities indicates that there are chromosome segregation problems, and further imply that embryos that fail to hatch likely die because of defective meiosis and consequential aneuploidy. Further supporting this, AMTA mutant oocytes display an increased frequency of univalent (achiasmatic) homologs at elevated temperatures, and this phenotype also increases dramatically in the presence of the *dc-1* transgene. The WT *syp-2::gfp* strain also has a slight increase in embryonic lethality and incidence of males at 25°C, suggesting that the GFP tag has a minor effect on SYP-2 function in synapsis. However, the AMTA *syp-2::gfp* strain has a significantly lower brood size than the WT *syp-2::gfp* and a higher frequency of males at all temperatures, and higher embryonic lethality at 20°C and 25°C, indicating that the GFP tag alone is not responsible for the AMTA *syp-2::gfp* phenotype. However, we cannot discount the possibility that the GFP also contributes to the genetic interaction with the *dlc-1* transgene. The increased phenotypes of the AMTA *syp-2* animals at 25°C correlates with decreased stability of the mutant protein at elevated temperatures, further supporting a proposed chaperone-like interaction with DLC-1 via the proposed DLC-1 interaction motif.

Window of SYP sensitivity

There appears to be a specific window in which SYP proteins can form aggregates after which they will assemble onto chromosomes. With short time periods at high temperatures, a small region of SYP aggregates is observed that grows as the high temperature is prolonged. All nuclei entering the transition zone after a shift down to a lower temperature exhibit normal SC assembly, while more advanced nuclei with aggregates do not recover (Bilgir et al. 2013). This indicates that there is a time within or near the end of the transition zone during which any onset of aggregation becomes irreversible. Post-translational modifications occurring before this point (e.g., phosphorylation and N-terminal acetylation of SYP proteins; Gao et al. 2016; Nadarajan et al. 2017; Sato-Carlton et al. 2018) could affect how SYP proteins interact and phase separate, and help the stabilize proper folding of, and interactions among, SYP proteins as synapsis begins to initiate (Rog et al. 2017). It has also been proposed that phase separation of the SC proteins occurs after assembly (Rog et al. 2017), and once the SYP proteins formed a stable CE, phase separation keeps them folded and/or interacting correctly. Conditions favoring aggregation at synapsis initiation could thus irreversibly prevent the stabilizing effects of phase separation. It is striking that male *C. elegans* do not require DLC-1 for normal synapsis. Males might add stabilizing post-translational modifications earlier than hermaphrodites or express other male-specific proteins to assist SYP folding. It is also possible that the increased speed of meiosis observed in males represents the absence of a delay in synapsis initiation (Jaramillo-Lambert et al. 2007), thus possibly bypassing any period where aggregation can occur.

Dynein light chain in early meiosis

Dynein light chains are hub proteins with many roles that are independent of the dynein motor (Rapali et al. 2011). In fact, DLC-1 has several other known motor independent roles in *C. elegans* germ cells. DLC-1 is needed to maintain the germline stem cell pool, by localizing FBF-2 to P-granules and promoting its function of suppressing translation of meiotic mRNAs (Wang et al. 2016). DLC-1 then promotes entry into meiosis by binding to GLD-1, which aids in the repression of some of GLD-1's target germline stem cell genes (Ellenbecker et al. 2019). In addition, DLC-1 promotes meiotic entry by both aiding in localization and function of the methyltransferase METT-10, which inhibits germline stem cell proliferation in sensitized backgrounds (Dorsett and Schedl 2009). We have further shown that DLC-1 may further have a chaperone-like function to help prevent inappropriate aggregation of SYP proteins before SC assembly is permitted, and this role is increasingly important with elevated temperature. These findings help to further characterize the complicated, multifaceted role of dynein light chain in protein interactions and meiosis.

Data availability

CRISPR-Cas9 constructed strains and RNAi plasmids used in this study are available upon request. Supplementary material is provided at figshare: <https://doi.org/10.25386/genetics.16918615>.

Acknowledgments

The authors would like to thank S. Nadajaran and M. Colaiaocovo for generous protocol consultation. They would also like to thank E. Voronina for the generous gift of the jmntSi13

[pME4.1] II; *dlc-1(tm3153)* strain, and A. Dernburg for the generous gift of the anti-SYP-1 antibody, S. Smolikov for the generous gift of the rabbit anti-SYP-2 antibody. They would like to thank S. L'Hernault and the members of the Kelly and Roger Deal labs for helpful experimental design suggestions.

Funding

This research was partially funded by the National Institute of General Medical Sciences of the National Institutes of Health under Award Number F31GM123750. This research was partially funded by the National Institutes of Health T32 training grant under the T32 GM008490.

Conflicts of interest

The authors declare that there is no conflict of interest.

Literature cited

- Bilgir C, Dombecki CR, Chen PF, Villeneuve AM, Nabeshima K. 2013. Assembly of the synaptonemal complex is a highly temperature-sensitive process that is supported by PGL-1 during *Caenorhabditis elegans* meiosis. *G3* 3(4):585–595.
- Bohr T, Nelson CR, Klee E, Bhalla N. 2015. Spindle assembly checkpoint proteins regulate and monitor meiotic synapsis in *C. elegans*. *J Cell Biol.* 211:233–242.
- Colaiaocovo MP, MacQueen AJ, Martinez-Perez E, McDonald K, Adamo A, et al. 2003. Synaptonemal complex assembly in *C. elegans* is dispensable for loading strand-exchange proteins but critical for proper completion of recombination. *Dev Cell.* 5:463–474.
- Couteau F, Nabeshima K, Villeneuve A, Zetka M. 2004. A component of *C. elegans* meiotic chromosome axes at the interface of homolog alignment, synapsis, nuclear reorganization, and recombination. *Curr Biol.* 14:585–592.
- Dorsett M, Schedl T. 2009. A role for dynein in the inhibition of germ cell proliferative fate. *Mol Cell Biol.* 29:6128–6139.
- Ellenbecker M, Osterli E, Wang X, Day NJ, Baumgarten E, et al. 2019. Dynein light chain DLC-1 facilitates the function of the Germline cell fate regulator GLD-1 in *Caenorhabditis elegans*. *Genetics.* 211:665–681.
- Gao J, Barroso C, Zhang P, Kim HM, Li S, et al. 2016. N-terminal acetylation promotes synaptonemal complex assembly in *C. elegans*. *Genes Dev.* 30:2404–2416.
- Goldstein P. 2013. Multiple synaptonemal complexes (polycomplexes) in wild-type hermaphroditic *Caenorhabditis elegans* and their absence in males. *Russ J Nematol.* 21:73–81.
- Goodyer W, Kaitna S, Couteau F, Ward JD, Boulton SJ, et al. 2008. HTP-3 links DSB formation with homolog pairing and crossing over during *C. elegans* meiosis. *Dev Cell.* 14:263–274.
- Harper NC, Rillo R, Jover-Gil S, Assaf ZJ, Bhalla N, et al. 2011. Pairing centers recruit a Polo-like kinase to orchestrate meiotic chromosome dynamics in *C. elegans*. *Dev Cell.* 21:934–947.
- Hodgkin J, Horvitz HR, Brenner S. 1979. Nondisjunction mutants of the nematode *Caenorhabditis elegans*. *Genetics.* 91:67–94.
- Hurlock ME, Cavka I, Kursel LE, Haversat J, Wooten M, et al. 2020. Identification of novel synaptonemal complex components in *C. elegans*. *J Cell Biol.* 219:e201910043.
- Jaramillo-Lambert A, Ellefson M, Villeneuve AM, Engebrecht J. 2007. Differential timing of S phases, X chromosome replication, and meiotic prophase in the *C. elegans* germ line. *Dev Biol.* 308:206–221.

- Kamath RS, Fraser AG, Dong Y, Poulin G, Durbin R, et al. 2003. Systematic functional analysis of the *Caenorhabditis elegans* genome using RNAi. *Nature*. 421:231–237.
- Lo KW, Naisbitt S, Fan JS, Sheng M, Zhang M. 2001. The 8-kDa dynein light chain binds to its targets via a conserved (K/R)XTQT motif. *J Biol Chem*. 276:14059–14066.
- Lui DY, Colaiacovo MP. 2013. Meiotic development in *Caenorhabditis elegans*. *Adv Exp Med Biol*. 757:133–170.
- MacQueen AJ, Colaiacovo MP, McDonald K, Villeneuve AM. 2002. Synapsis-dependent and -independent mechanisms stabilize homolog pairing during meiotic prophase in *C. elegans*. *Genes Dev*. 16:2428–2442.
- Makokha M, Hare M, Li M, Hays T, Barbar E. 2002. Interactions of cytoplasmic dynein light chains Tctex-1 and LC8 with the intermediate chain IC74. *Biochemistry*. 41:4302–4311.
- Nadarajan S, Lambert TJ, Altendorfer E, Gao J, Blower MD, et al. 2017. Polo-like kinase-dependent phosphorylation of the synaptonemal complex protein SYP-4 regulates double-strand break formation through a negative feedback loop. *Elife*. 6:e23437.
- Nadarajan S, Mohideen F, Tzur YB, Ferrandiz N, Crawley O, et al. 2016. The MAP kinase pathway coordinates crossover designation with disassembly of synaptonemal complex proteins during meiosis. *Elife*. 5:e12039.
- Nyarko A, Hare M, Hays TS, Barbar E. 2004. The intermediate chain of cytoplasmic dynein is partially disordered and gains structure upon binding to light-chain LC8. *Biochemistry*. 43:15595–15603.
- Page SL, Hawley RS. 2001. c(3)G encodes a *Drosophila* synaptonemal complex protein. *Genes Dev*. 15:3130–3143.
- Penkner A, Tang L, Novatchkova M, Ladurner M, Fridkin A, et al. 2007. The nuclear envelope protein Matefin/SUN-1 is required for homologous pairing in *C. elegans* meiosis. *Dev Cell*. 12:873–885.
- Phillips CM, Dernburg AF. 2006. A family of zinc-finger proteins is required for chromosome-specific pairing and synapsis during meiosis in *C. elegans*. *Dev Cell*. 11:817–829.
- Phillips CM, Wong C, Bhalla N, Carlton PM, Weiser P, et al. 2005. HIM-8 binds to the X chromosome pairing center and mediates chromosome-specific meiotic synapsis. *Cell*. 123:1051–1063.
- Rapali P, Szenes A, Radnai L, Bakos A, Pal G, et al. 2011. DYNLL/LC8: a light chain subunit of the dynein motor complex and beyond. 278:2980–2996.
- Rodriguez-Crespo I, Yelamos B, Roncal F, Albar JP, Ortiz de Montellano PR, et al. 2001. Identification of novel cellular proteins that bind to the LC8 dynein light chain using a pepscan technique. *FEBS Lett*. 503:135–141.
- Rog O, Dernburg AF. 2015. Direct visualization reveals kinetics of meiotic chromosome synapsis. *Cell Rep*. 10:1639–1645.
- Rog O, Kohler S, Dernburg AF. 2017. The synaptonemal complex has liquid crystalline properties and spatially regulates meiotic recombination factors. *Elife*. 6:e21455.
- Sato A, Isaac B, Phillips CM, Rillo R, Carlton PM, et al. 2009. Cytoskeletal forces span the nuclear envelope to coordinate meiotic chromosome pairing and synapsis. *Cell*. 139:907–919.
- Sato-Carlton A, Nakamura-Tabuchi C, Chartrand SK, Uchino T, Carlton PM. 2018. Phosphorylation of the synaptonemal complex protein SYP-1 promotes meiotic chromosome segregation. *J Cell Biol*. 217:555–570.
- Schild-Prufert K, Saito TT, Smolikov S, Gu Y, Hincapie M, et al. 2011. Organization of the synaptonemal complex during meiosis in *Caenorhabditis elegans*. *Genetics*. 189:411–421.
- Smolikov S, Eizinger A, Schild-Prufert K, Hurlburt A, McDonald K, et al. 2007. SYP-3 restricts synaptonemal complex assembly to bridge paired chromosome axes during meiosis in *Caenorhabditis elegans*. *Genetics*. 176:2015–2025.
- Smolikov S, Schild-Prufert K, Colaiacovo MP. 2009. A yeast two-hybrid screen for SYP-3 interactors identifies SYP-4, a component required for synaptonemal complex assembly and chiasma formation in *Caenorhabditis elegans* meiosis. *PLoS Genet*. 5: e1000669.
- Wagner W, Fodor E, Ginsburg A, Hammer JA, III, 2006. The binding of DYNLL2 to myosin Va requires alternatively spliced exon B and stabilizes a portion of the myosin's coiled-coil domain. *Biochemistry*. 45:11564–11577.
- Wang X, Olson JR, Rasoloson D, Ellenbecker M, Bailey J, et al. 2016. Dynein light chain DLC-1 promotes localization and function of the PUF protein FBF-2 in germline progenitor cells. *Development*. 143:4643–4653.
- Wynne DJ, Rog O, Carlton PM, Dernburg AF. 2012. Dynein-dependent processive chromosome motions promote homologous pairing in *C. elegans* meiosis. *J Cell Biol*. 196:47–64.
- Zhang L, Ward JD, Cheng Z, Dernburg AF. 2015. The auxin-inducible degradation (AID) system enables versatile conditional protein depletion in *C. elegans*. *Development*. 142:4374–4384.

Communicating editor: J. Engebrecht